The endocytic catalysts, Rab5a and Rab7, are tandem regulators of thyroid hormone production

Karine Croizet-Berger*, Chantal Daumerie†, Marianne Couvreur*, Pierre J. Courtoy*, and Marie-France van den Hove*†‡

*Cell Biology Unit, Christian de Duve Institute of Cellular Pathology, and †Endocrinology Department, Université Catholique de Louvain, B-1200 Brussels, Belgium

Rab proteins are small GTPases that control distinct vesicular transport steps. Along the endocytic pathway, Rab5a is a rate-limiting catalyst of internalization, and Rab7 controls trafficking through late endosomes to lysosomes. The dependence of thyroid hormone production by thyrocytes on thyroglobulin endocytosis and intracellular processing in late endosomes/lysosomes suggests that its rate can be regulated by the expression or function of these endocytic catalysts. We compared the expression level and membrane recruitment of Rab5a and Rab7 in autonomous thyroid adenomas (where the cAMP cascade is constitutively activated) and surrounding quiescent tissues. The concentrations of Rab5a and Rab7, but not of Rab8, were coordinately increased up to 6-fold in adenomas, and correlated with a proportionate decrease in soluble thyroglobulin content (reflecting colloid depletion by accelerated endocytic uptake in hyperactive tissue). In adenomas, a higher proportion of Rab5a and Rab7 was membrane associated, and the equilibrium density of particulate Rab7 and iodine shifted toward lysosomal fractions, indicating that progression along the degradation pathway also was promoted. In cultures of polarized human thyrocytes from normal patients, thyroid-stimulating hormone or forskolin increased, to a similar extent, Rab5a and Rab7 but not Rab8 expression, apical endocytosis of thyroglobulin and lucifer yellow, and basolateral secretion of T_3 and T_4. Taken together, these *in vivo* and *in vitro* observations demonstrate that thyroid-stimulating hormone, via cAMP, coordinately enhances the expression of Rab5a and Rab7, which promote Tg endocytosis and transfer to lysosomes, respectively, resulting in accelerated thyroid hormone production.

The synthesis and secretion of thyroid hormones are tightly regulated processes that involve a well defined sequence of events. First, thyroglobulin (Tg), the macromolecular thyroid hormone precursor, is secreted at the apical pole of thyroid cells in the follicular lumen. In this storage compartment, Tg undergoes posttranslational modifications leading to the intramolecular formation of T_3 and T_4 hormonogenic residues. Next, mature Tg undergoes endocytosis at the apical membrane and is transferred to early, then to late, endosomes and to lysosomes, where Tg is believed to be degraded with the release of free thyroid hormones (for a review, see ref. 1). However, demonstration of proteolytic release of selected hormonogenic residues before transport to lysosomes indicates that Tg degradation may involve two sequential compartments, i.e., late endosomes and lysosomes, respectively (2). In thyrocytes, Tg endocytosis and hormone secretion are stimulated by thyroid-stimulating hormone (TSH) via a cAMP-dependent pathway (3). However, the downstream effectors triggering Tg endocytosis and transport toward proteolytic compartments are not identified. Because both Tg substrate in the follicular lumen and hydrolytic enzymes in late endosomes/lysosomes are in vast excess (4), we hypothesized that thyroid hormone production is regulated by the encounter of substrate and hydrolases, i.e., that it depends on rate-limiting endocytic catalysts.

Endocytic uptake, vesicular transport, and membrane fusion events are regulated by Rab proteins, a family of Ras-like small GTPases composed of 60 members in humans (5, 6). Rab proteins shuttle between cytosol and membranes and cycle between an inactive GDP- and an active GTP-bound form. Cytosolic GDP-bound Rab protein, complexed to Rab GDP-dissociation inhibitor (GDI; ref. 7), is presented to the donor membrane where dissociation of GDI may be facilitated by a displacement factor (8). GDP/GTP nucleotide exchange occurs upon Rab protein recruitment to the membrane and is regulated by guanine nucleotide exchange factors (GEFs; ref. 9). After membrane fusion with acceptor membrane, GTPase activating factors (GAPs) interact with Rab protein to stimulate GTP hydrolysis and Rab inactivation (10). Inactivated GDP-bound Rab protein is recognized by GDI for release from membrane and recycling.

Along the endocytic pathway, Rab5 and Rab7 are considered as the key regulators. Rab5 is a rate-limiting catalyst of the endocytic uptake and delivery to early endosomes of both fluid-phase and receptor-mediated endocytic tracers, as well as of homotypic endosomal fusion (11, 12). All of these events are indeed slowed down by overexpression of defective Rab5 mutants acting as dominant-negative (Rab5 S34N or Rab5 N133I) and are conversely accelerated by overexpression of wild-type Rab5a acting as dominant-positive (12–15). In the same way, the constitutively active Rab5 mutant, Rab5-Q79L, causes the enlargement of endosomes and accelerates fluid-phase and receptor-mediated endocytosis (13, 15). Rab7, located on the late endocytic compartments, functions downstream of Rab5 and has been involved in the fusion of late endocytic structures; more recently, it has been involved in the biogenesis and maintenance of the lysosomal compartment (16–18). Dominant-negative Rab7 slows down degradation of low-density lipoprotein (LDL), but dominant-positive Rab7 alone is not sufficient to accelerate this process (17), suggesting that coordinate expression of both Rab5a and Rab7 might be required to bring endocytic substrates down to the degradative compartment by tandem action.

In the thyroid gland, nothing is known about the role of Rab proteins in the endocytic uptake and processing of Tg and their regulation according to the thyroid metabolism. Because Tg endocytosis and hormone secretion are stimulated by TSH or cAMP, we postulated that the expression of endocytic catalysts such as Rab5a and Rab7 could be regulated by the TSH/cAMP cascade. To test this hypothesis, we have compared the expression level and subcellular distribution of Rab5a and Rab7 in hyper- and hypoactive thyroid tissue from the same patients and in polarized thyrocytes *in vitro* upon treatment by TSH or the adenylate cyclase activator, forskolin. For the first aim, we took advantage of thyroid autonomous adenomas (AA), benign encapsulated tumors that actively metabolize iodine and secrete thyroid hormones independently of the normal control of TSH.

MEDICAL SCIENCES

In Europe, the vast majority of thyroid AA result from constitutive activation of the cAMP cascade because of mutations in the TSH receptor gene; for a small number of patients, mutations in the G protein genes lead to the same effects (19, 20).

We found that the level of expression of Rab5a and Rab7 in AAs was both coordinately increased and inversely related to the follicular Tg content, an index of colloid depletion by endocytic uptake. Furthermore, activation of the thyroid gland increased membrane recruitment of both catalysts and shifted subcellular location of particulate Rab7 and iodine toward distal compartments of the late endocytic apparatus, where hydrolytic enzymes are more concentrated. Finally, in cultured polarized thyrocytes, cAMP also increased Rab5a and Rab7 expression and accelerated apical endocytosis of Tg as well as basolateral secretion of thyroid hormones. These results strongly suggest that endocytic uptake and intracellular trafficking of Tg are rate-limiting steps in thyroid hormone production and are triggered in tandem by increased expression of the endocytic catalysts, Rab5a and Rab7, in response to cAMP.

Materials and Methods

Patients and Tissues. Nine euthyroid patients bearing AAs were selected for this study based on identification of hot nodule by scintigraphy, partly or completely suppressed activity in perinodular (PN) tissue, and very low ($n = 4$) or undetectable serum TSH level ($n = 5$). Paired samples of the encapsulated AAs and adjacent PN tissues were obtained by surgery. Two patients had received iodine before surgery (patients 2 and 7), one was treated with β-adrenergic antagonists (patient 2), and none had taken antithyroid drugs. For the culture of polarized human thyrocytes, normal tissue was dissected from patients undergoing surgery for cold nodules. The study was approved by the Ethical Committee of the University of Louvain, Medical School.

Analytical subcellular fractionation was performed as described (21, 22). Briefly, samples of nodular and PN tissue were homogenized in 10 volumes of ice-cold 250 mM sucrose/10 mM Tris, pH 7.4 and sequentially centrifuged at $400 \times g$ for 10 min, at $30,000 \times g$ for 7.5 min, and $134,000 \times g$ for 45 min, to isolate nuclei and cell debris (N fraction), large particles (ML fraction), and microsomes (P fraction) and the final supernatant (S), respectively. ML fractions were mixed with 22.6% (wt/vol) Percoll (Amersham Pharmacia) in 250 mM sucrose/10 mM Tris, pH 7.4 and further resolved by centrifugation at $53,600 \times g$ for 30 min. Twenty fractions, collected from the bottom, were either assayed for proteins and iodine content after Percoll pelleting or were directly analyzed by marker enzyme assays and Western blotting.

Isolation and Culture of Human Polarized Thyrocytes. Open thyroid follicles were isolated by enzymatic digestion of normal human tissue as described (23) and suspended in Coon's-modified Ham F-12 medium containing 5% (vol/vol) FCS, 100 units/ml penicillin, 50 μg/ml streptomycin, and 2.5 μg/ml fungizone (all from GIBCO) and fortified by 175 nM insulin/65 nM human transferrin/10 μM hydrocortisone/6 nM somatostatin/25 nM glycyl-L-histidyl-L-lysine acetate (all from Sigma). Cells were plated at 0.6×10^6 cells per cm² in Transwell 3412 inserts (Costar) precoated with type I collagen (Roche Diagnostics) and cultured under 5% CO₂ at 37°C. Culture medium was renewed every other day. After 5–7 days, when transepithelial resistance exceeded 1,000 $\Omega \times$ cm² (Millicell ERS ohmmeter, Millipore), bovine TSH or forskolin (both from Sigma) was added to the basolateral medium as indicated. Cells were further incubated for 4 days in the same conditions, except that insulin was omitted from apical and basolateral media during the last day of culture to eliminate spurious effects of insulin on Rab5 (24). At the time

of the experiment, transepithelial electric resistance was always above 1,500 $\Omega \times$ cm².

[¹²⁵I]Thyroglobulin and Fluid-Phase Endocytosis. To measure Tg endocytosis, 50 nM [¹²⁵I]thyroglobulin was added to the apical medium (0.5–0.7 μCi per insert; 1 Ci = 37 GBq), and the basolateral medium was replaced by Tyrode buffer enriched by 10 mM Tris, pH 7.4/1 mM NaClO₄/0.5% (wt/vol) BSA, supplemented or not by TSH or forskolin, as appropriate. After 2 h of incubation at 37°C, filters were placed on ice and washed 3× in ice-cold PBS containing 2 mM Ca²⁺, 3× in PBS-Ca²⁺ supplemented by 1% (wt/vol) BSA, and 3× in PBS-Ca²⁺ for 30 s each. Cells were scraped off the filter in ice-cold PBS by using a rubber policeman, centrifuged at $150 \times g$ for 5 min at 4°C, rinsed once with PBS, and resuspended in buffer A [150 mM NaCl/125 mM Tris, pH 7.4, containing 1 mM EGTA and protease inhibitors (Complete, Roche Molecular Biochemicals)]. Cell-associated radioactivity was measured in a γ-counter. To determine Tg internalization, [¹²⁵I]Tg binding to thyrocytes after 2 h of incubation at 4°C was measured in parallel ($\approx$30% of values at 37°C) and was subtracted as background.

To assay for fluid-phase endocytosis, lucifer yellow lithium salt (Sigma) was added to the apical medium to reach 2 mg/ml. After 2 h at 37°C or 4°C (for control), cells were washed 3× with ice-cold PBS containing 0.1% (wt/vol) BSA and 4× with ice-cold PBS, for 30 s each. Cells then were scraped off the filter, lysed in ice-cold PBS containing 0.05% (vol/vol) Triton X-100, and sonicated for 15 s. Fluorescence was determined in a Packard FluoroCount (Packard) with λ_{exc} at 426 nm and λ_{em} at 530 nm, normalized to a lucifer yellow standard curve in the same medium, and expressed as volume of medium cleared by fluid-phase endocytosis. There was no detectable uptake at 4°C.

Thyroid Hormone Secretion. Thyrocyte monolayers were washed and incubated for 18 h at 37°C in serum-free Coon's medium containing 10 μM nonradioactive thyroglobulin in the apical medium and 0.1% (wt/vol) ovalbumin (Sigma) supplemented or not by TSH or forskolin in the basolateral medium. The latter was collected, and the content of free T_3 and T_4 was determined by RIA as described by the manufacturer (Biocode, Liège, Belgium).

Western Blotting. Filter-cultured thyrocytes (collected in buffer A and sonicated for 15 s) and homogenates or subcellular fractions were resolved by SDS/12% PAGE and transferred onto polyvinylidene fluoride membrane (NEN). After blocking for 2 h at room temperature with 2% (wt/vol) BSA and 0.5% (vol/vol) Tween-20 in 150 mM NaCl/5 mM EDTA/20 mM Tris, pH 7.4, membranes were probed overnight at 4°C with rabbit antisera against either Rab5a (1:200, Santa Cruz Biotechnology) or Rab7 (1:2,000, kindly provided by M. Zerial, Max-Planck Institute, Dresden, Germany), or mouse monoclonal antibodies against Rab8 (1:100, Transduction Laboratories, Lexington, KY). After washing, blots were incubated with peroxidase-conjugated secondary antibodies (Amersham Pharmacia) followed by enhanced chemiluminescence detection (NEN). For strict comparison, samples of seven pairs were rerun in parallel on the same gel, and the analysis was repeated three times. Signals were quantified by using NIH IMAGE V.1.62 program and related to DNA content (21).

Analytical Procedures. Protein content was determined by reference to BSA by using Lowry's procedure for homogenates, subcellular fractions, and cell lysates, and by using Bio-Rad reagent for Percoll gradient fractions. Iodine, DNA, 5'-nucleotidase activity, and cathepsin D and B activities were measured as reported (21, 25). Colloid thyroglobulin concentration in the homogenates was calculated from the proportion
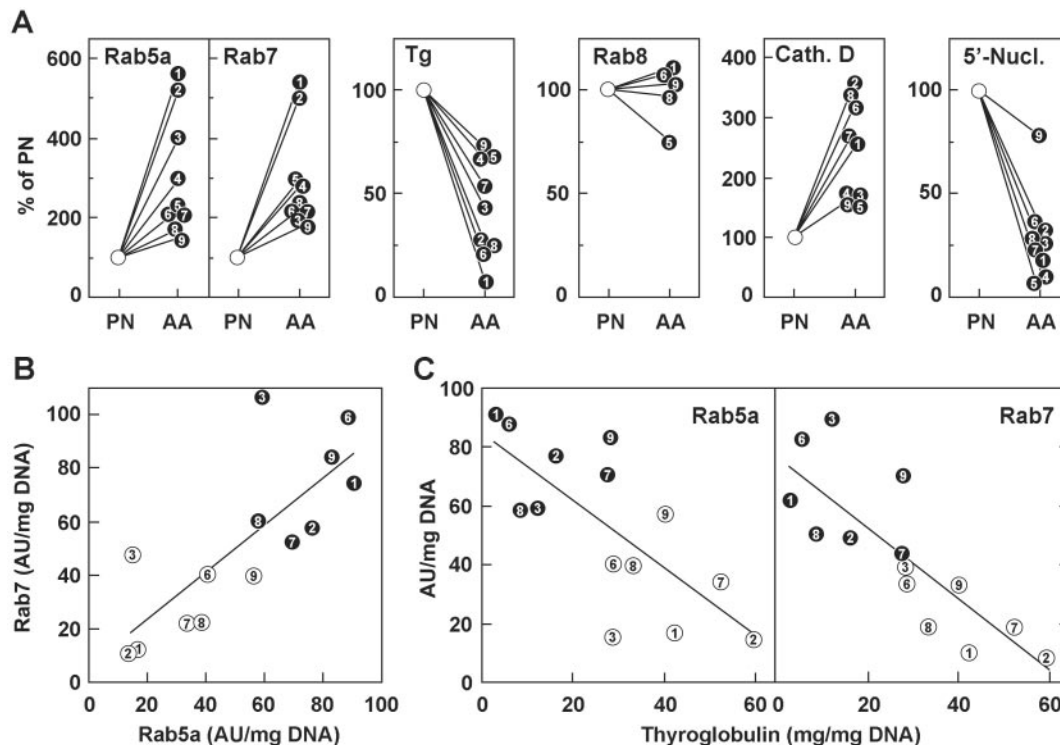
Fig. 1. The coordinate increase in Rab5a and Rab7 levels inversely correlates with residual Tg content, according to the thyroid gland activation state. Homogenates from nodular AA and PN tissues of nine patients (each identified by a different number) were analyzed for Rabs (Western blotting) and Tg content (see *Materials and Methods*). Cathepsin D (lysosomal marker) and 5′-nucleotidase (apical membrane marker) activities were assayed in parallel. All values were normalized per mg DNA. (*A*) Specific content or activity in AA were expressed as a percentage of corresponding PN tissues. (*B* and *C*) Correlation in AA (filled circles) and corresponding PN tissues (white circles) between individual levels of Rab5a and Rab7, measured (*B*) on the same blot ($r = 0.77$, $P < 0.01$) or (*C*) between Tg content and Rab5a ($r = -0.74$, $P < 0.01$) or Rab7 ($r = -0.82$, $P < 0.001$). Samples from patients 4 and 5 were not available for this analysis.

of 19 S Tg in the high-speed supernatant (21). Human nonradioactive Tg was purified either from a goiter of a patient with a Pendred syndrome (endocytosis experiments) or from a normal thyroid tissue (secretion experiments), as reported (21). Tg (3 nmol) with a low level of iodination (2 mol iodine/mol Tg) was labeled *in vitro* with 2 mCi ^{125}I (IMS30, Amersham Pharmacia) together with 75 nmol nonradioactive iodine, by 200 milliunits lactoperoxidase (Calbiochem) and 60 milliunits glucose oxidase (Roche Molecular Biochemicals) in 0.2 ml of 10 mM glucose/20 mM phosphate buffer, pH 7.2 for 2 h at 37°C. After a new round of purification as 19 S Tg by sucrose gradient and dialysis in Tyrode fortified by 10 mM Tris buffer, pH 7.4, the product was found to contain 20 mol ^{125}I/mol Tg, of which 7–8% was recovered as T$_3$ and 20% as T$_4$ after pronase hydrolysis (21).

Statistical Analysis. Nonparametric Wilcoxon's ranking test was used, except when stated otherwise.

Results

Rab5a and Rab7 Expression Level Increases with the Activation State of the Thyroid Tissue. The rate of endocytic uptake and trafficking to lysosomes, which presumably governs thyroid hormone production, depends on Rab5 and Rab7, respectively. Therefore, we first compared by Western blotting the expression level of Rab5a and Rab7 in homogenates of hyperactive AAs and surrounding quiescent tissues from nine patients. For control, Rab8, which is involved in the secretory but not in the endocytic pathway, was measured in parallel. As an index of endocytic activity, colloid depletion was estimated by the decrease of soluble Tg concentration. Cathepsin D was selected as a lysosomal marker enzyme because it is involved in the proteolytic release of thyroid hormones (4), and 5′-nucleotidase was used as a marker of apical

plasma membrane. As shown in Fig. 1*A*, levels of Rab5a and Rab7, but not of Rab8, were increased 1.5- to 6-fold in all AAs by reference to corresponding PN tissues, while soluble Tg concentration was decreased in comparable proportions. Cathepsin D activity also increased in active tissues, although to a lesser extent, and 5′-nucleotidase activity dramatically decreased in eight of nine adenomas. Moreover, when comparing values between individual patients on the same blot, Rab5a and Rab7 levels correlated with one another (Fig. 1*B*) and showed a significant inverse correlation with soluble Tg concentration (Fig. 1*C*). These results suggested that Rab5a and Rab7 expression was coordinately induced upon TSH-receptor activation, and that increased concentration of Rab5a caused a proportionate acceleration of Tg endocytosis.

Recruitment of Rab5a and Rab7 to Particulate Fractions Is Increased in the Hyperactive Adenomatous Tissue. Because Rabs shuttle between an inactive cytosolic pool and a membrane-associated active pool, particulate and soluble fractions were prepared by differential centrifugation of homogenates from nodular and PN tissues, and the distributions of Rab5a and Rab7 were compared with those of cathepsin D and B (Fig. 2). Surprisingly, in resting tissue, Rab5a and Rab7 were predominantly found in the high-speed supernatant (i.e., cytosol: $59 \pm 13\%$ and $56 \pm 19\%$, $n = 3$, respectively). Recruitment onto membranes in adenomas was moderately increased for Rab5a and for Rab7, and Rab5a became preferentially recruited onto large particles (ML fraction; for the three parameters, ≈ 1.5-fold; $P < 0.05$); Rab7 was increasingly recruited on both large (ML fraction) and small particles (P fraction). Cathepsin B was essentially found in ML fractions in both resting and activated tissues; cathepsin D was mostly retrieved in the high-speed supernatant in resting tissues
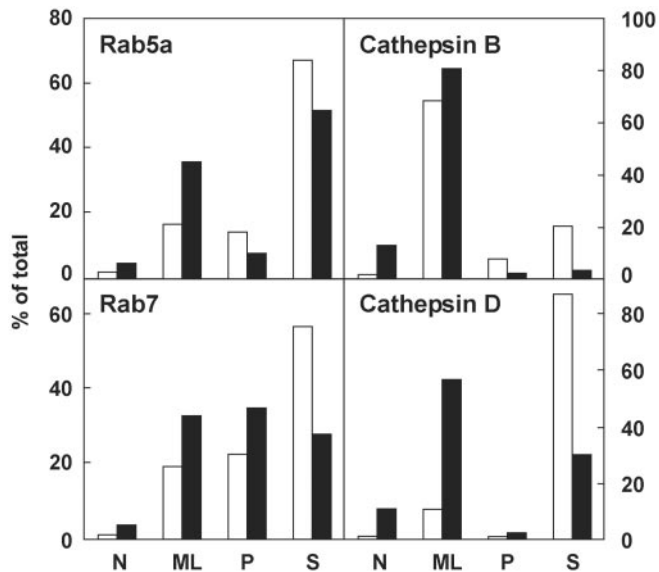
Fig. 2. Increased particulate recruitment of Rab5a and Rab7 in AAs. Four fractions obtained by differential centrifugation of thyroid homogenates (N, nuclear; ML, large particles; P, small particles; and S, soluble) from PN (white bars) and AA tissues (black bars) were analyzed for Rab5a and Rab7 (Western blotting) and for cathepsin B and D (enzyme activities). Results were expressed as percentages of the homogenate. Figure shows a representative pair of the three (Rabs) or nine (enzymes) analyzed.

but became preferentially associated with large particles (ML fraction) in adenomas. Altogether, these results indicated that, in addition to triggering the expression of both catalysts, thyrocyte stimulation led to activation of Rab5a and Rab7 and improved cathepsin D retention, as reflected by increased particulate recruitment.

Rab5a and Rab7 Expression Levels Correlate with Iodine Accumulation in Dense Lysosomes. To define further the subcellular compartments to which Rab5a and Rab7 associate, and to test whether increased levels and activation of Rab5a and Rab7 would favor transfer of Tg from colloid to lysosomes, ML fractions from adenomas and PN tissues were further resolved in Percoll density gradients. As expected, the plasma membrane marker, 5′ nucleotidase, was essentially confined to the lighter fractions (pools I and II in Fig. 3A) and lysosomal markers, cathepsin B and D, peaked in dense fractions (pool IV) in both resting and active tissues. Upon thyrocyte activation, particulate iodine shifted from pool II to pool IV, indicating accelerated transfer of Tg to dense lysosomes. Rab5a was broadly distributed in pools I-III. The distribution of Rab7 was shifted from the intermediate-density pools II and III in resting tissue to denser fractions, including pool IV, in hyperactive tissues. When comparing paired samples, the enrichment of iodine in the lysosomal fractions (pool IV) correlated with the expression level of Rab5a and Rab7 in the homogenates (Fig. 3B). Taken together, these results suggested that thyrocyte activation caused redistribution of Rab7 toward more distal compartments of the endocytic apparatus concomitantly with accelerated transfer of Tg into lysosomes.

In Vitro, the TSH/cAMP Cascade Is Sufficient to Induce Rab5a and Rab7 Expression and to Accelerate Thyroglobulin Endocytosis and Thyroid Hormone Production. To test whether the TSH/cAMP cascade would produce the same effects *in vitro*, human thyrocytes isolated from normal tissue were established as tightly polarized epithelia on a permeable support (23). Thyrocytes coordinately
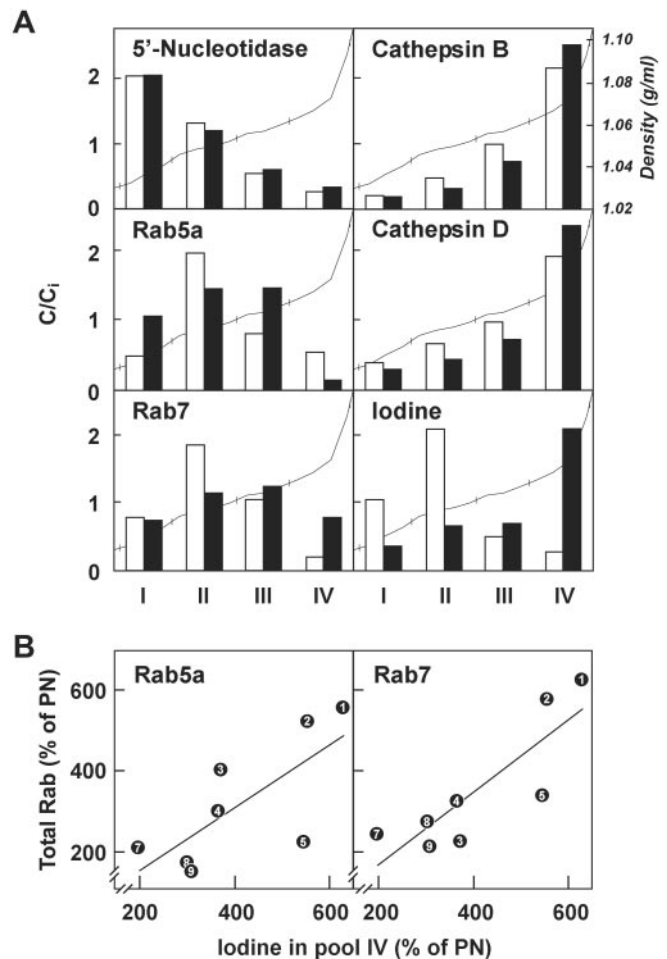

Fig. 3. (A) Density distributions in Percoll gradients. Particulate (ML) fractions from PN (white bars) and AA tissues (black bars) were mixed with Percoll and centrifuged. Pooled fractions are shown for the sake of simplicity (I, 1.032–1.052 in density; II, 1.052–1.056; III, 1.057–1.060; IV, 1.063–1.097). For each pool, content is expressed with respect to the initial content before centrifugation (C/Ci). Results are from one representative of the three analyzed. The shape of the gradient is superimposed (thin line). (B) Correlation between the increased content for Rab5a and Rab7 in total homogenates and for iodine in dense lysosomes (ML fraction, pool IV), in AA tissues with respect to corresponding PN tissues. Rab5a: $r = 0.73$, $P < 0.05$; Rab7: $r = 0.84$, $P < 0.01$.

responded to basolateral addition of TSH or forskolin for 4 days by an ≈2-fold increase in (*i*) expression of Rab5a and Rab7 (Fig. 4A); (*ii*) apical endocytosis of [^{125}I]Tg and lucifer yellow (Fig. 4B); and (*iii*) basolateral secretion of free thyroid hormones upon apical addition of unlabeled Tg (Fig. 4C). On the contrary, no change in Rab8 expression was observed (data not shown). Endocytic accumulation of the large tracer, Tg, was at least 3-fold higher than for the small molecular weight tracer, lucifer yellow, pointing to an adsorptive component in Tg uptake (26). Knowing the T_3 and T_4 content of the internalized Tg, the efficiency of conversion of prohormone into free hormones recovered in the basolateral medium (reflecting polarized secretion) could be estimated at 3.7% h^{-1} for T_3 and 0.6% h^{-1} for T_4 in the absence of stimulation. For T_3, the efficiency of conversion was increased ≈2-fold upon TSH or forskolin treatment. The preference in T_3 over T_4 release upon stimulation can easily be explained by the action of type II iodothyronine deiodinase and its well known activation by TSH in the human thyroid (27). Altogether, *in vitro* stimulation of the TSH/cAMP
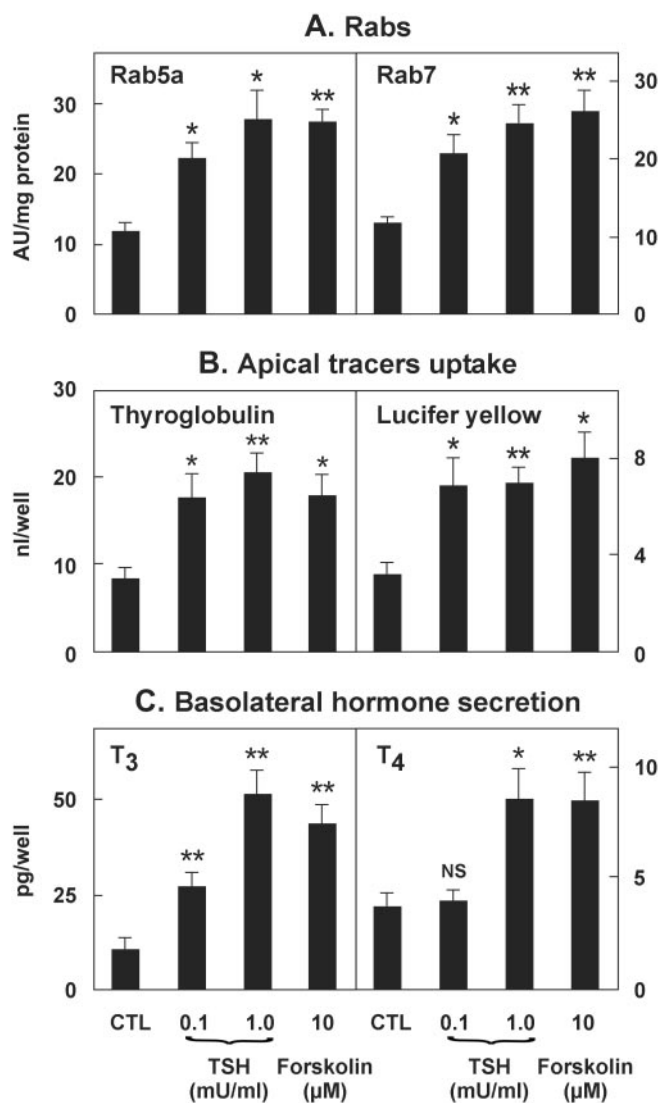
Croizet-Berger *et al*.

A. Rabs

B. Apical tracers uptake

C. Basolateral hormone secretion

Fig. 4. Expression of Rab5a and Rab7, apical endocytosis, and thyroid hormone secretion are up-regulated *in vitro* by cAMP. In this representative experiment of three, polarized monolayers of thyrocytes from a normal thyroid gland (see *Materials and Methods*) were treated or not for 4 days with TSH or forskolin, as indicated. Cells then were allowed to internalize 50 nM radiolabeled Tg or 2 mg/ml lucifer yellow from the apical medium for 2 h at 37°C; cells then were washed, lysed, and tracer uptake was expressed as nl cleared per well (*B*). Alternatively, cells were incubated with 10 μM nonradioactive Tg in the apical medium for 18 h at 37°C, after which basolateral medium was collected for thyroid hormones assay (*C*). Aliquots of cell lysates then were analyzed for Rab5a and Rab7 content by Western blotting (*A*). Data are means ± SEM of four wells. Statistical analysis by unpaired Student's *t* test: *, $P < 0.05$; **, $P < 0.01$; NS, not significant.

cascade reconstituted the key findings of AAs: increased expression of rate-limiting endocytic catalysts leading to accelerated Tg endocytosis and conversion into thyroid hormones.

Discussion

This report shows that the expression of Rab5a and Rab7, which catalyze endocytosis and vesicular transport toward lysosomes respectively, is coordinately regulated by TSH both *in vivo* and *in vitro*. As compared with corresponding PN tissues, expression levels of both catalysts is indeed increased up to 6-fold in AAs, where the cAMP regulatory cascade is constitutively activated. This effect is specific, because Rab8 is not affected, and func-

tionally significant, because the increase of expression of both catalysts correlates linearly with Tg endocytosis, as reflected by colloid depletion. Second, in hyperactive tissues, a higher proportion of Rab5a and Rab7 is recruited onto membranes, and Rab7 is redistributed onto dense lysosomes that also harbor a higher proportion of particulate iodine. Third, the use of polarized human thyrocytes confirmed that Rab5a and Rab7 expression is induced either by TSH or by forskolin, with a parallel acceleration in apical endocytosis of Tg and basolateral secretion of thyroid hormones, thereby demonstrating the regulatory role of the cAMP signal-transduction pathway.

It is generally accepted that Rab5 controls the rate of endocytosis (12–15). Indeed, the kinetics of fluid-phase and receptor-mediated endocytosis is accelerated ≈2.5-fold in heterologous systems such as baby hamster kidney (BHK) cells transfected with wild-type dog Rab5 when overexpressed ≈15-fold but not when overexpressed ≈5-fold (12). In addition, rat liver sinusoidal cells show both faster endocytic kinetics and higher Rab5 expression than hepatocytes on a cell protein basis, although the relation to a cell number basis was not clear (28). Downstream of Rab5, Rab7 specifically regulates transfer toward lysosomes. Indeed, transfection of BHK cells with dominant-negative mutants of dog Rab7 markedly inhibits degradation of low-density lipoproteins (LDL), whereas the internalization rate is unaffected (17). Noticeably, in cells transfected either with wild-type Rab5 or constitutively active Rab7 alone, LDL degradation is not accelerated (17), implying that both catalysts are required to act in tandem to bring extracellular proteins down to lysosomes. The present study, which deals not only with a homologous system but also with the same cell type, shows the coordinate regulation of Rab5a and Rab7 and strongly suggests that their tandem action accelerates Tg endocytosis and transfer into the proteolytic compartment where thyroid hormones are produced. Moreover, this response is not limited to pathological tissues, because TSH treatment of normal human thyrocytes also induces both catalysts. The lack of comparable Rab8 variations suggests that the increase in Rab5a and Rab7 content does not simply result from an overall prolongation of Rab proteins half-life; it points to a coordinated control of transcription. Database screening (with MATINSPECTOR) identifies potential cAMP response element in the promoter sequences of both Rab5a and Rab7 genes.

In quiescent thyroid tissues, Rab5a and Rab7 are mainly soluble and, thus, probably belong to a GDI-associated, GDP-bound inactive cytosolic pool. This finding is in marked contrast with transfected BHK or Madin-Darby canine kidney cell lines overexpressing Rab5 or Rab7, in which Rab proteins were reported to be essentially recovered in membrane fractions (11, 29). On the other hand, AAs show increased membrane association of Rab5a and Rab7, as well as redistribution of Rab7 toward lysosomes. Three aspects of the Rab cycle could modulate Rab membrane recruitment: Rab geranylgeranylation, GDI sequestration, and GDP exchange/GTP hydrolysis.

First, geranylgeranylation is necessary for Rab membrane association and could be enhanced upon activation of Rab geranylgeranyltransferase, as evidenced in response to IFN-γ (30) or insulin (31), but never reported so far in response to cAMP. Second, in BHK cells, induction of the mitogen-activated protein kinase (MAPK) p38 upon oxidative stress promotes Rab5 dissociation from membranes by catalyzing GDI phosphorylation, concomitantly with acceleration of fluid-phase endocytosis (32). This finding leads to the suggestion that availability of cytosolic Rab5-GDI complex may be rate limiting for endocytosis. In human thyrocytes, TSH stimulates p38 MAPK (33) and H_2O_2 production (34). Therefore, if the same mechanism would operate in thyrocytes as reported for BHK cells, one would expect a decreased membrane association of Rab5, but the converse was found. One possible explanation for

this discrepancy is the much larger cytosolic pool in thyrocytes under basal conditions than in transfected cell lines. Alternatively, activation of GDI might facilitate delivery of Rab-GDP to distinct active membrane domains along the degradation pathway (35).

Third, membrane recruitment and, possibly, redistribution to downstream compartments depend on the guanine nucleotide state of Rab proteins, as shown in HeLa cells where a dominant-positive, GTPase-defective mutant of Rab7 reaches lysosomes (18, 36). The guanine nucleotide state can be regulated by GAP or GEF activities. One obvious candidate is p120 Ras GAP, which can physically interact with Rab5a and stimulate its GTPase activity (37); this interaction is sensitive to pharmacological treatment (38). Other candidates are the GEFs, Rabex-5, Rin1, and Epac. Rabex-5 physically associates with Rab5a together with the effector Rabaptin-5. Rin1 interacts with the GDP-bound Rab5a and stimulates epidermal growth factor receptor endocytosis (39). Nevertheless, modulation of these factors by cAMP has not been reported (9). Conversely, Epac is regulated by cAMP, but its interaction with Rab proteins remains speculative (40).

Finally, increased expression of Rab7 could favor the formation of the hybrid organelles between late endosomes and lysosomes (41) or their conversion into dense lysosomes. The shift of particulate iodine (reflecting iodo amino acids of Tg) from endosomes in PN tissues toward lysosomes in AAs, supports the hypothesis that Tg processing and thyroid hormone release can already occur in late endosomes of quiescent thyrocytes with moderate efficiency, as observed upon aging (22). In contrast, Tg processing by active cells is essentially achieved by lysosomes resulting in accelerated hormone production, as found in stimulated thyroid remnants (21).

1. Björkman, U. & Ekholm, R. (1990) in *The Thyroid Gland*, ed. Greer, M. A. (Raven, New York), pp. 83–125.
2. Rousset, B., Selmi, S., Bornet, H., Bourgeat, P., Rabilloud, R. & Munari-Silem, Y. (1989) *J. Biol. Chem.* **264,** 12620–12626.
3. Vassart, G. & Dumont, J. E. (1992) *Endocr. Rev.* **13,** 596–611.
4. Dunn, A. D., Crutchfield, H. E. & Dunn, J. T. (1991) *Endocrinology* **128,** 3073–3080.
5. Somsel-Rodman, J. & Wandinger-Ness, A. (2000) *J. Cell Sci.* **113,** 183–192.
6. Zerial, M. & McBride, H. (2001) *Nat. Rev. Mol. Cell Biol.* **2,** 107–117.
7. Pfeffer, S. R., Dirac-Svejstrup, A. B. & Soldati, T. (1995) *J. Biol. Chem.* **270,** 17057–17059.
8. Dirac-Svejstrup, A. B., Sumizawa, T. & Pfeffer, S. R. (1997) *EMBO J.* **16,** 465–472.
9. Horiuchi, H., Lippe, R., McBride, H. M., Rubino, M., Woodman, P., Stenmark, H., Rybin, V., Wilm, M., Ashman, K., Mann, M., *et al.* (1997) *Cell* **90,** 1149–1159.
10. Xiao, G. H., Shoarinejad, F., Jin, F., Golemis, E. A. & Yeung, R. S. (1997) *J. Biol. Chem.* **272,** 6097–6100.
11. Gorvel, J. P., Chavrier, P., Zerial, M. & Gruenberg, J. (1991) *Cell* **64,** 915–925.
12. Bucci, C., Parton, R. G., Mather, I. H., Stunnenberg, H., Simons, K., Hoflack, B. & Zerial, M. (1992) *Cell* **70,** 715–728.
13. Li, G. & Stahl, P. D. (1993) *J. Biol. Chem.* **268,** 24475–24480.
14. Li, G., Barbieri, M. A., Colombo, M. I. & Stahl, P. D. (1994) *J. Biol. Chem.* **269,** 14631–14635.
15. Stenmark, H., Parton, R. G., Steele-Mortimer, O., Lutcke, A., Gruenberg, J. & Zerial, M. (1994) *EMBO J.* **13,** 1287–1296.
16. Feng, Y., Press, B. & Wandinger-Ness, A. (1995) *J. Cell Biol.* **131,** 1435–1452.
17. Vitelli, R., Santillo, M., Lattero, D., Chiariello, M., Bifulco, M., Bruni, C. B. & Bucci, C. (1997) *J. Biol. Chem.* **272,** 4391–4397.
18. Bucci, C., Thomsen, P., Nicoziani, P., McCarthy, J. & van Deurs, B. (2000) *Mol. Biol. Cell* **11,** 467–480.
19. Parma, J., Duprez, L., Van Sande, J., Hermans, J., Rocmans, P., Van Vliet, G., Costagliola, S., Rodien, P., Dumont, J. E. & Vassart, G. (1997) *J. Clin. Endocrinol. Metab.* **82,** 2695–2701.
20. Deleu, S., Allory, Y., Radulescu, A., Pirson, I., Carrasco, N., Corvilain, B., Salmon, I., Franc, B., Dumont, J. E., Van Sande, J., *et al.* (2000) *Thyroid* **10,** 131–140.
21. van den Hove, M. F., Couvreur, M., Col, V., Gervy, C., Authelet, M. & Neve, P. (1995) *Eur. J. Cell Biol.* **68,** 437–445.
22. van den Hove, M. F., Couvreur, M., Authelet, M. & Neve, P. (1998) *Cell Tissue Res.* **294,** 125–135.
23. Nilsson, M., Husmark, J., Nilsson, B., Tisell, L. E. & Ericson, L. E. (1996) *Eur. J. Endocrinol.* **135,** 469–480.
24. Huang, J., Imamura, T. & Olefsky, J. M. (2001) *Proc. Natl. Acad. Sci. USA* **98,** 13084–13089.
25. Limet, J. N., Quintart, J., Schneider, Y. J. & Courtoy, P. J. (1985) *Eur. J. Biochem.* **146,** 539–548.
26. Lemansky, P. & Herzog, V. (1992) *Eur. J. Biochem.* **209,** 111–119.
27. Murakami, M., Araki, O., Hosoi, Y., Kamiya, Y., Morimura, T., Ogiwara, T., Mizuma, H. & Mori, M. (2001) *Endocrinology* **142,** 2961–2967.
28. Juvet, L. K., Berg, T. & Gjoen, T. (1997) *Hepatology* **25,** 1204–1212.
29. Chavrier, P., Parton, R. G., Hauri, H. P., Simons, K. & Zerial, M. (1990) *Cell* **62,** 317–329.
30. Alvarez-Dominguez, C. & Stahl, P. D. (1998) *J. Biol. Chem.* **273,** 33901–33904.
31. Goalstone, M. L., Leitner, J. W., Golovchenko, I., Stjernholm, M. R., Cormont, M., Le Marchand-Brustel, Y. & Draznin, B. (1999) *J. Biol. Chem.* **274,** 2880–2884.
32. Cavalli, V., Vilbois, F., Corti, M., Marcote, M. J., Tamura, K., Karin, M., Arkinstall, S. & Gruenberg, J. (2001) *Mol. Cell* **7,** 421–432.
33. Pomerance, M., Abdullah, H. B., Kamerji, S., Correze, C. & Blondeau, J. P. (2000) *J. Biol. Chem.* **275,** 40539–40546.
34. Corvilain, B., Laurent, E., Lecomte, M., Vansande, J. & Dumont, J. E. (1994) *J. Clin. Endocrinol. Metab.* **79,** 152–159.
35. Sonnichsen, B., De Renzis, S., Nielsen, E., Rietdorf, J. & Zerial, M. (2000) *J. Cell Biol.* **149,** 901–914.
36. Meresse, S., Gorvel, J. P. & Chavrier, P. (1995) *J. Cell Sci.* **108,** 3349–3358.
37. Liu, K. & Li, G. (1998) *J. Biol. Chem.* **273,** 10087–10090.
38. Chen, X. & Wang, Z. (2001) *EMBO Rep.* **2,** 842–849.
39. Tall, G. G., Barbieri, M. A., Stahl, P. D. & Horazdovsky, B. F. (2001) *Dev. Cell* **1,** 73–82.
40. de Rooij, J., Zwartkruis, F. J., Verheijen, M. H., Cool, R. H., Nijman, S. M., Wittinghofer, A. & Bos, J. L. (1998) *Nature (London)* **396,** 474–477.
41. Mullock, B. M., Bright, N. A., Fearon, C. W., Gray, S. R. & Luzio, J. P. (1998) *J. Cell Biol.* **140,** 591–601.